ELSEVIER

Journal of Medical Imaging and Radiation Sciences xx (2017) 1-11

Journal of Medical Imaging and Radiation Sciences

Journal de l'imagerie médicale et des sciences de la radiation

www.elsevier.com/locate/jmir

The Acceptability of Iterative Reconstruction Algorithms in Head CT: An Assessment of Sinogram Affirmed Iterative Reconstruction (SAFIRE) vs. Filtered Back Projection (FBP) Using Phantoms

Martine A. Harris, MSc[a*], John Huckle, EdD[b], Denis Anthony, PhD[b] and Paul Charnock, MSc[c]

[a] *Radiology Department, Mid Yorkshire Hospitals NHS Trust, Pinderfields General Hospital, Wakefield, UK*
[b] *School of Healthcare, Faculty of Medicine and Health, University of Leeds, Leeds, UK*
[c] *Integrated Radiological Services Ltd., Liverpool, UK*

ABSTRACT

Background: Computed tomography (CT) is the primary imaging investigation for many neurologic conditions with a proportion of patients incurring cumulative doses. Iterative reconstruction (IR) allows dose optimization, but head CT presents unique image quality complexities and may lead to strong reader preferences.

Objectives: This study evaluates the relationships between image quality metrics, image texture, and applied radiation dose within the context of IR head CT protocol optimization in the simulated patient setting. A secondary objective was to determine the influence of optimized protocols on diagnostic confidence using a custom phantom.

Design: Experimental design.

Methods and setting: A three-phase phantom study was performed to characterize reconstruction methods at the local reference standard and a range of exposures. CT numbers and pixel noise were quantified supplemented by noise uniformity, noise power spectrum, contrast-to-noise ratio (CNR), high- and low-contrast resolution. Reviewers scored optimized protocol images based on established reporting criteria.

Results: Increasing strengths of IR resulted in lower pixel noise, lower noise variance, and increased CNR. At the reference standard, the image noise was reduced by 1.5 standard deviation and CNR increased by 2.0. Image quality was maintained at $\leq$24% relative dose reduction. With the exception of image sharpness, there were no significant differences between grading for IR and filtered back projection reconstructions.

Conclusions: IR has the potential to influence pixel noise, CNR, and noise variance (image texture); however, systematically optimized IR protocols can maintain the image quality of filtered back projection. This work has guided local application and acceptance of lower dose head CT protocols.

RÉSUMÉ

Contexte : La tomodensitométrie (TDM) est la principale étude d'imagerie pour plusieurs problèmes neurologiques et une certaine proportion de patients reçoivent des doses cumulatives. La reconstruction itérative (RI) permet d'optimiser la dose, mais la TDM de la tête présente des complexités uniques sur le plan de la qualité des images et pourrait conduire à de fortes préférences de la part du lecteur.

Objectifs : L'étude évalue les relations entre les mesures de qualité de l'image; la texture de l'image et la dose de rayonnement appliquée dans le contexte de l'optimisation du protocole de TDM en RI de la tête dans un environnement de patient simulé. Un objectif secondaire était de déterminer l'influence des protocoles optimisés sur le degré de confiance du diagnostic à l'aide d'un fantôme personnalisé.

Conception : Une étude sur fantôme en trois phases a été effectuée afin de caractériser les méthodes de reconstruction à la norme de référence locale et à différentes expositions. Les données de TDM et le bruit de pixel ont été quantifiés et compléments par uniformité du bruit, spectre de puissance du bruit, ratio contraste/bruit et résolution de contraste élevée et faible. Les examinateurs ont noté les images des protocoles optimisés selon les critères de présentation établis.

Résultats : L'augmentation de la force de la RI s'est traduite par une réduction du bruit de pixel, une variance plus basse du bruit et une augmentation du ratio contraste/bruit. À la norme de référence, le bruit de l'image était réduit de 1,5 écart-type et le ratio

* Corresponding author: Martine. A. Harris, MSc, Radiology Department, Mid Yorkshire Hospitals NHS Trust, Pinderfields General Hospital, Aberford Road, Wakefield WF1 4DG, UK.
E-mail address: martine.harris@midyorks.nhs.uk (M.A. Harris).

1939-8654/$ - see front matter
http://dx.doi.org/10.1016/j.jmir.2017.04.002

contraste/bruit était augmenté de 2,0 écarts types. La qualité de l'image a été maintenue à ≤24% de réduction de la dose relative. À l'exception de la netteté de l'image, il n'y a eu aucune différence significative en gradation entre la RI et les reconstructions par rétroprojection des projections filtrées (FBP).

Conclusions : La RI a le potentiel d'influence le bruit de pixel, le ratio contraste/bruit et la variance du bruit (texture de l'image); cependant, des protocoles de RI systématiquement optimisés peuvent maintenir la qualité d'image de la reconstruction FBP. Cette étude a guidé l'application locale et l'acceptation des protocoles de TDM de la tête à dose plus basse.

Introduction

Computed tomography (CT) is the primary imaging investigation for a range of neurologic conditions [1], with many studies performed acutely for the detection of intracranial hemorrhage in stroke and trauma [2]. A proportion of patients require multiple head CT studies over the course of treatment, incurring cumulative dose [3]. Dose optimization based upon objective and subjective image quality measures remains central to radiation safety. This is of particular importance with the advent of dose-reduction technology and the opportunity to influence image quality in the raw data domain, rather than purely at the postprocessing stage.

Traditional filtered back projection (FBP) methods yield noisy images, susceptible to artifacts dependent on the reconstruction filters and radiation doses applied [4], but theoretically iterative reconstruction (IR) allows optimization of dose and image quality [5] through noise and artifact minimization [6]. The most common hybrid IR algorithms perform an initial weighted FBP reconstruction prior to IR noise removal to maintain familiar image appearances [7]. However, applying denoising and regularization with IR can alter the edge of structures and image texture [8–11]. Many studies have compared image quality between FBP and IR, and it has been recognized that dose reduction with IR algorithms is highly dependent on the individual CT systems [12], the clinical task, and the requirement for low-contrast resolution imaging [10].

The published literature is conflicting as to whether IR techniques can preserve low-contrast resolution as radiation dose is decreased [13]. This is of particular significance in head CT due to beam hardening through the skull base and the necessity for excellent grey and white matter differentiation [6]. In comparison to FBP, the noise-free appearance and over-smoothing of critical structures with IR can be detrimental when detecting subtle pathologic changes [14].

For clinical departments, the diverse principles of IR and FBP techniques, variations between vendors and confidentiality of denoising algorithms, may result in IR CT data sets that appear different from traditional FBP images. In neuroradiology, this has led to strong reader preferences not encountered in most body applications, reported lower levels of diagnostic confidence [14] and nonacceptance for local clinical implementation within dose-reduction strategies. The current study follows suggestions that introducing IR protocols within a controlled research setting can be beneficial [13].

The main purpose of this study was to evaluate the relationships between image quality metrics, image texture, and applied radiation dose within the context of IR head CT protocol optimization in the simulated patient setting. A secondary objective was to implement the maximum level of IR while maintaining similar image quality to determine the influence of optimized protocols on diagnostic confidence using a custom phantom.

Materials and Methods

Imaging phantoms were utilized in this three-phase experimental study to closely reproduce the clinical scenario and allow control of scan parameters in multiple acquisitions. Institutional approvals were obtained prior to CT acquisition and recruitment of human participants for image review (University Ref: SHREC/RP/389). The reviewers provided written consent to participate following study explanation and comprised four individuals experienced in head CT interpretation.

Phantoms

Phase 1 utilized an anthropomorphic Alderson-Rando brain phantom (The Phantom Laboratory, Greenwich, NY) to collect CT number and image (pixel) noise information for both reconstruction algorithms. To supplement, in phase 2, CT performance data were acquired in accordance with the American College of Radiology guidelines [15] using a Gammex 463 image quality phantom (Gammex, Inc., Middleton, WI). Phase 3 attempted to simulate head CT image interpretation using an early iteration of a prototype phantom (Leeds Test Objects Ltd., Boroughbridge, UK). With a design specification defined by the investigator for this discrete study and informed by literature review and clinical measurements of CT density, this prototype phantom utilized various urethane rubber concentrations to simulate the attenuation values of common acute intracranial pathologies (Figure 1).

Scan Parameters

CT acquisitions were performed using a Siemens Somatom Definition AS, 128-slice, single-source scanner (Siemens AG, Forcheim, Germany). Acquisition and reconstruction parameters are listed in Table 1. In phases 1 and 2, imaging phantoms were scanned with the institutional reference standard protocol and 12 consecutive acquisitions of reduced tube current-time combination. As recommended in previous research, automated tube-current modulation was utilized to identify maximum dose-reduction levels [16, 17]. Images

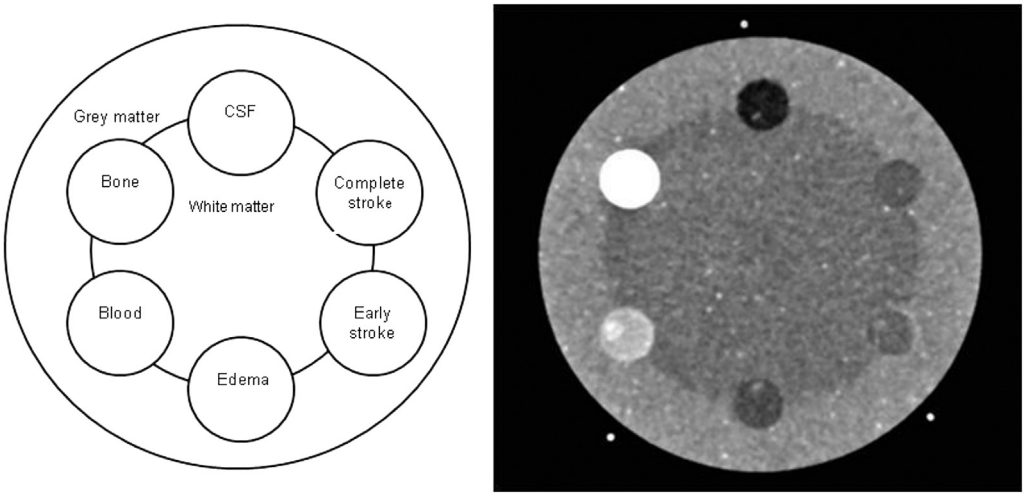

Figure 1. Prototype phantom representing normal anatomy and acute intracranial pathology. CSF, cerebrospinal fluid.

were reconstructed with FBP and IR medium smooth convolution kernels. For each exposure, IR images were reconstructed using the five SAFIRE iteration strength settings which influence the level of noise reduction and image texture [7]. The custom phantom utilized in phase 3 was scanned with the full-dose reference standard protocol (FBP reconstruction) and four optimized exposure protocols. These were identified in preceding phases as having comparable objective image quality to the reference standard, defined as equivalent image noise and ±10% of the reference standard contrast-to-noise ratio (CNR).

Effective milliampere-second (mAs) which is known to be linearly related to dose was altered exclusively without modification of tube potential or scan length, and relative dose has therefore been reported rather than effective dose. The CT dose index for the scanned volume and dose length product for each effective mAs combination in phase 1 was also documented.

Table 1
Scan and Reconstruction Parameters

Variable	Phase 1	Phase 2	Phase 3
Phantom	Rando	Gammex	Custom
kV	120	120	120
Eff. mAs	410–290	410–290	410, 370, 350, 310
Pitch	0.55	0.55	0.55
Gantry rotation time, s	1.0	1.0	1.0
Collimation, mm	0.6	0.6	0.6
Care Dose 4D	Yes	Yes	Yes
SFOV, cm	25	25	25
DFOV, mm	215	215	215
Matrix size	512 × 512	512 × 512	512 × 512
Slice thickness, mm	5	5	5
Reconstruction algorithm, FBP/IR	H40s/J40s	H40s/J40s	H40s/J40s

DFOV, display field of view; Eff. mAs, effective milliampere-second; FBP, filtered back projection; IR, Iterative reconstruction; SFOV, scan field of view.

Image Quality Analysis

In phase 1, quantitative measurements were made by the principal investigator from a Siemens Syngo workstation (Siemens AG, Forcheim, Germany). To quantify pixel noise, a 1-cm^2 region of interest (ROI) was consistently positioned using a grid on axial FBP and IR images. Partial-voluming artifacts were avoided during ROI placement. Density values were recorded as the mean CT number in Hounsfield units (HU) and image noise by means of the standard deviation (SD). For each reconstruction algorithm and exposure, measures were repeated three times and averaged.

Image noise and uniformity were measured from phantom images acquired in phase 2 with CT numbers of peripheral ROIs checked that they remain within ±5 HU of the central mean HU [15]. To describe the variance and spatial frequency content of noise for each reconstruction process, noise power spectrum (NPS) curves were produced from the uniform module using Image Quality works (version 0.7, Sourceforge.net). Within the low-contrast module, two 1.0-cm^2 ROIs were placed on the largest low-contrast material insert and on the background material in each image. Measurements were taken three times and averaged to determine CNR using formula [15]:

$$CNR = \frac{CT\ \ number(lowcontrast) - CT\ \ number(background)}{Standard\ \ deviation(background)}$$

Subjective assessments of image contrast were performed independently by two reviewers in a randomized and blinded manner on picture archiving and communication system workstations (Agfa-Gevaert N.V. Mortsel, Belgium). Low-contrast resolution was judged by the number of low-contrast cylinder sets visible. The maximum spatial frequency was measured by the number of high-contrast resolution bar patterns which could be sharply discriminated [15].

Further subjective image quality assessments were made on five images obtained in phase 3 by four reviewers (each with a

minimum of 8-year experience of reporting CT head examinations independently). Blinded images were randomly allocated and reviewed on standardised window settings to mimic the clinical scenario (80WW/40WL). Images were reviewed for image noise and sharpness, artifacts, pathology, lesion conspicuity, diagnostic confidence, and acceptability. Reviewer's responses were recorded on a bespoke data collection tool using Likert scales informed by previous studies [16, 18, 19]. The grading system was adapted from the Guidelines on Quality Criteria for Computed Tomography [20], where lower mean scores for each quality criterion indicate better image quality.

Statistical Analysis

SPSS was used for statistical analysis (IBM SPSS Statistics, version 22). A two-way random intraclass correlation coefficient (ICC) was used for absolute agreement between reviewers for subjective low-contrast visibility. Analysis of variance (ANOVA) was used to compare mean image scores for quality criteria during multirater review. Post hoc testing for pairwise comparison of means was performed when a statistically significant finding was identified. A P value of $<.05$ was considered to be statistically significant.

Results

The reference standard protocol reconstructed with FBP produced a mean CT number of 33.2 HU and image noise of 3.3 SD. Across the tested clinical exposure range, CT numbers for FBP and all SAFIRE strengths remained within ±2 HU. Although the relationship between exposure and noise was consistent between reconstructions, this was not quadratic for FBP or SAFIRE (Figure 2). For the same x ray, tube current increasing the iteration strength linearly decreased image noise, while CT number remained within ±1 HU. Pixel noise measurements for iteration strengths 1 and 2 demonstrated results within 10% of the reference FBP protocol, but SAFIRE strengths 3–5 produced pixel noise levels ≤3 SD.

From the 12 effective mAs combinations explored in phase 1, four exposure levels reconstructed with FBP and IR provided pixel image noise equivalent to that currently preferred by locally (reference standard protocol). These "optimized" exposure protocols and the reference standard were utilized in phase 3 with random image numbers assigned to resultant images acquired with each protocol (Table 2). A maximum of 100 effective mAs reduction resulted in a 16.77 mGy reduction in CT dose index for the scanned volume and 281 mGy cm reduction of dose length product. They represent a maximum 24% relative dose reduction for SAFIRE reconstruction and 10% for FBP.

Within the Gammex phantom, noise uniformity was within ±5 HU for all reconstructions and exposure levels. Generally, for a given radiation dose, optimized SAFIRE reconstructions had higher CNR than that of FBP and CNR progressively increased with higher strengths of SAFIRE (Figure 3). This trend was seen across all clinical exposure levels tested. SAFIRE strengths 1 and 2 provided comparable CNR measurements to the reference standard protocol at lower exposures.

The NPS curves compare the optimized and reference standard protocols (Figure 4) and demonstrate that stochastic noise levels decreased as the strength of SAFIRE increased. NPS curves for low IR strengths showed minimal reduction in the mean spatial frequency of the resultant noise, maintaining a coarse graininess, although FBP was superior with increase in span at frequencies between 0.2 and 0.4 cycles per millimetre (c/mm).

There was 100% agreement between two reviewers for subjective assessment of high-contrast resolution; four lines of circular bar patterns representing ≤7 line pairs per centimetre (lp/cm) were resolved in each image regardless of acquisition and reconstruction protocol. With regard to low-contrast resolution, increased subjective object visibility was seen with higher exposures and SAFIRE strengths. The different acquisition and reconstruction protocols accounted for low reviewer reliability (ICC [single], .194; [95% confidence interval: −.046, −.409] and ICC [multiple], .325; [95% confidence interval: −.096, −.581]).

Images of the prototype phantom were individually assessed and marked for diagnostic image quality by reviewers. There were statistically significant differences in mean values for grading of image sharpness ($P < .001$), lesion conspicuity ($P = .004$), diagnostic acceptability ($P = .011$) criteria, and for total scores ($P = .009$) (Table 3). There was no significant difference in image noise ($P = .152$), image artifacts ($P = .977$), or in diagnostic confidence scoring when identifying simulated pathologies ($P = .379$).

The greatest variation in mean scores for optimized protocols was observed for image sharpness (Figure 5). The image acquired at 370 effective mAs FBP (Figure 6B) was graded best for image sharpness characteristics. No statistically significant difference in image sharpness was identified with lower dose IR reconstructions (Figure 6C-E), which were considered superior to the full-dose FBP reference standard (Figure 6A) and inferior to 370 effective mAs FBP.

There was a significant difference between the means of the full-dose FBP reference standard (Figure 6A) and 370 effective mAs FBP (Figure 6B) when scoring diagnostic acceptability ($P = .023$) and lesion conspicuity ($P = .009$). No significant differences in means were demonstrated between scores for FBP and SAFIRE reconstructions when considering diagnostic acceptability and lesion conspicuity criteria.

Image quality criteria scores were combined to generate a result of total diagnostic ability (Figure 7). Post hoc testing showed an overall significant difference between means for full-dose and reduced-dose FBP reconstruction ($P = .013$) scores represented by images 3 and 4 (Figure 7). There was no significant difference in means and an identified overlap in score ranges for lower dose FBP and IR exposure protocols (Figure 7—images 1, 2, 4, and 5).

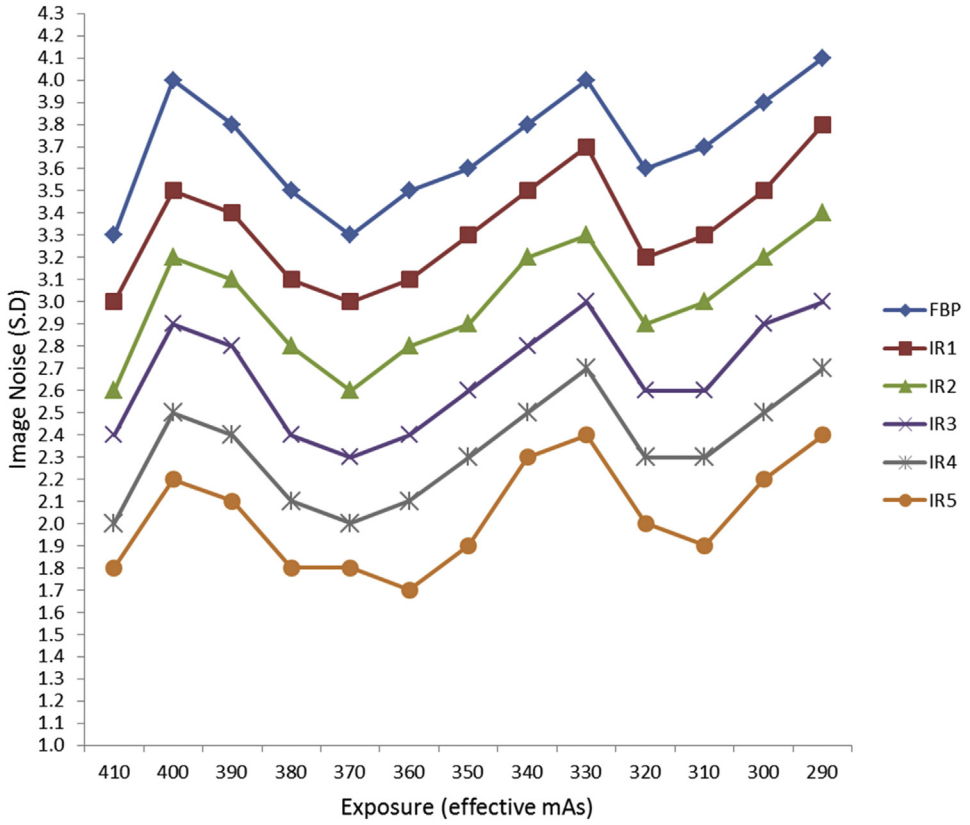

Figure 2. The relationship between exposure and image noise with FBP and different strengths of IR measured in the Rando phantom. FBP, filtered back projection; IR, iterative reconstruction; mAs, milliampere-second.

Discussion

This work compares FBP and SAFIRE methods by exploring phantom images at different photon count levels. The use of phantoms to regulate initial IR algorithm settings has been explored previously [18, 21]. Low strength SAFIRE reconstructions compensated for reductions in radiation exposure and produced objective image quality metrics similar to those obtained with full-dose FBP. Noise and uniformity within all image acquisition protocols also conformed to the requirements of the American College of Radiology [15]. In agreement with a previous study utilizing a Catphan image quality phantom [22], image quality assessment demonstrated that CT numbers were not affected by IR settings.

Equivalent image quality was achievable with FBP at 10% relative dose reduction supporting the notion that the institutional reference standard exposure was greater than that required for diagnostic purposes. It is well documented in the literature that due to the visual subjectivity of CT image quality, the application of radiation doses greater than those required for maximum diagnostic information can be inadvertently applied [13]. Increasing radiation exposure beyond the point of image quality optimization for the anatomic area of interest and clinical question does not provide additional information to the human observer. Although all images reviewed in this study had the same values for objective image quality measures, the quality of the institutional reference standard protocol images was judged inferior than those of optimized protocols owing to perceived levels of subjective image sharpness and the ability to detect low-contrast lesions.

Table 2
Dose Metrics and Image Randomization of the Institution Reference Standard and "Optimized Image Protocols"

Exposure Protocol	Eff. mAs Reduction	Relative Dose Reduction (%)	CTDIVol (mGy)	DLP (mGy cm)	Image Randomization
410 mAs FBP (reference)	—	—	70.18	1174	Image 3
370 mAs FBP	40	9.76	63.66	1065	Image 4
350 mAs IR 1	60	14.63	59.94	1002	Image 5
330 mAs IR 2	80	19.51	56.52	945	Image 2
310 mAs IR 1	100	24.39	53.41	893	Image 1

CTDIvol, computed tomography dose index volume; DLP, dose length product; Eff. mAs, effective milliampere-second; FBP, filtered back projection; IR, iterative reconstruction; mAs, milliampere-second.

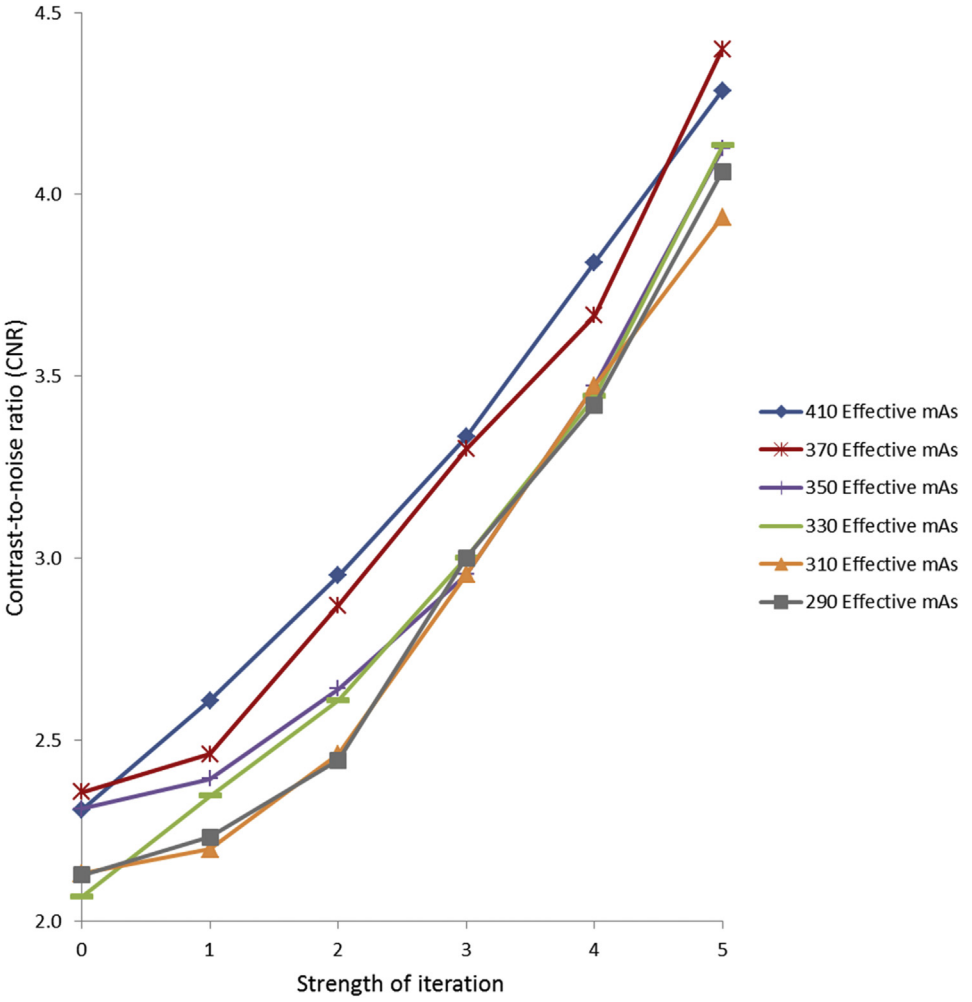

Figure 3. The relationship between reconstruction technique and CNR at maximum, minimum, and optimized tested radiation exposure levels in the Gammex phantom. Iteration strength zero represents FBP. CNR, contrast-to-noise ratio; FBP, filtered back projection; mAs, milliampere-second.

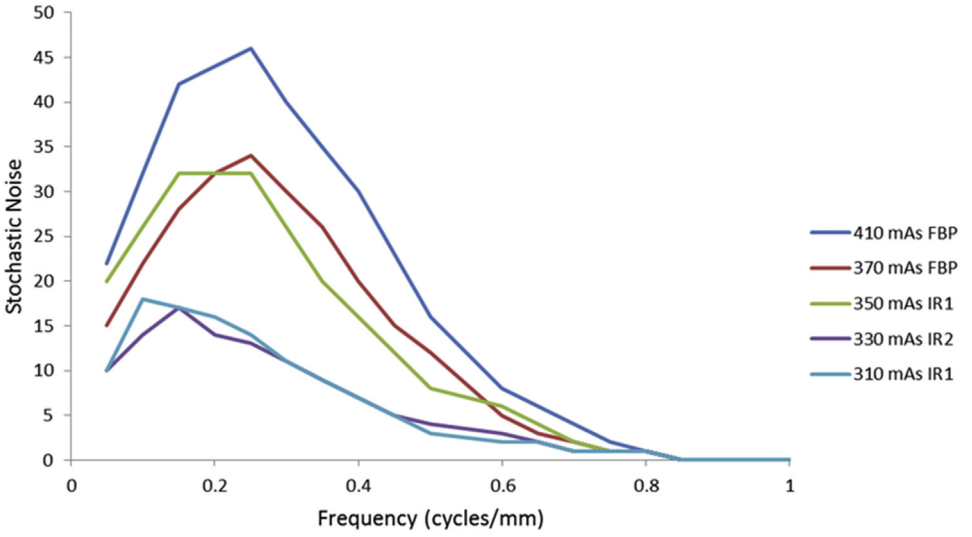

Figure 4. NPS curves for the institution reference standard and optimal protocols identified in phases 1 and 2. FBP, filtered back projection; IR, iterative reconstruction; mAs, milliampere-second; NPS, noise power spectrum.

Table 3
ANOVA Demonstrating Differences in Means for the Institution Reference Standard (410 eff. mAs FBP) and Four Optimized Image Protocols When Assessed for CT Quality Criteria

Subjective Variable	*P* Value	Post hoc Analysis Group Differences	Mean Differences	Sig.
Image sharpness	.000	330 eff. mAs IR 1 and 410 eff. mAs FBP	−1.500	.011
		310 eff. mAs IR 1 and 370 eff. mAs FBP	1.250	.038
		410 eff. mAs FBP and 370 eff. mAs FBP	2.250	.000
		410 eff. mAs FBP and 350 eff. mAs IR 2	1.250	.038
Image noise	.152	—	—	—
Artifacts	.977	—	—	—
Diagnostic confidence	.379	—	—	—
Lesion conspicuity	.004	410 eff. mAs FBP and 370 eff. mAs FBP	2.000	.009
Diagnostic acceptability	.011	410 eff. mAs FBP and 370 eff. mAs FBP	1.250	.023
Total score	.009	410 eff. mAs FBP and 370 eff. mAs FBP	7.250	.013

ANOVA, analysis of variance; CT, computed tomography; Eff. mAS, effective milliampere-second; FBP, filtered back projection; IR, Iterative reconstruction; Sig, significance.

Importantly, consistent with other research [16, 18, 19, 23, 24], the findings indicate a potential maximum relative dose-reduction limit of up to 24% for head CT examinations with SAFIRE reconstruction. However, other institutions prefer to practice on the side of caution and report only 15% dose reduction for CT head [25]. With the combination of novel dose-reducing strategies such as model-based reconstruction methods [22, 26] and noise efficient detectors [27], there is likely to be further significant dose reduction in the future.

Unlike other IR studies [5, 11, 16, 18, 19, 21, 23, 24] in both phantoms and patients, a quadratic relationship was not observed between exposure and image noise; this may be due to the use of dose modulation or type and strength of filters and kernels applied by the vendor to optimize the image quality at various detector photon counts. Unfortunately, this denoising information is not accessible to the end user.

Low interrater reliability was observed for perceived low-contrast detectability attributed to the exposure level and

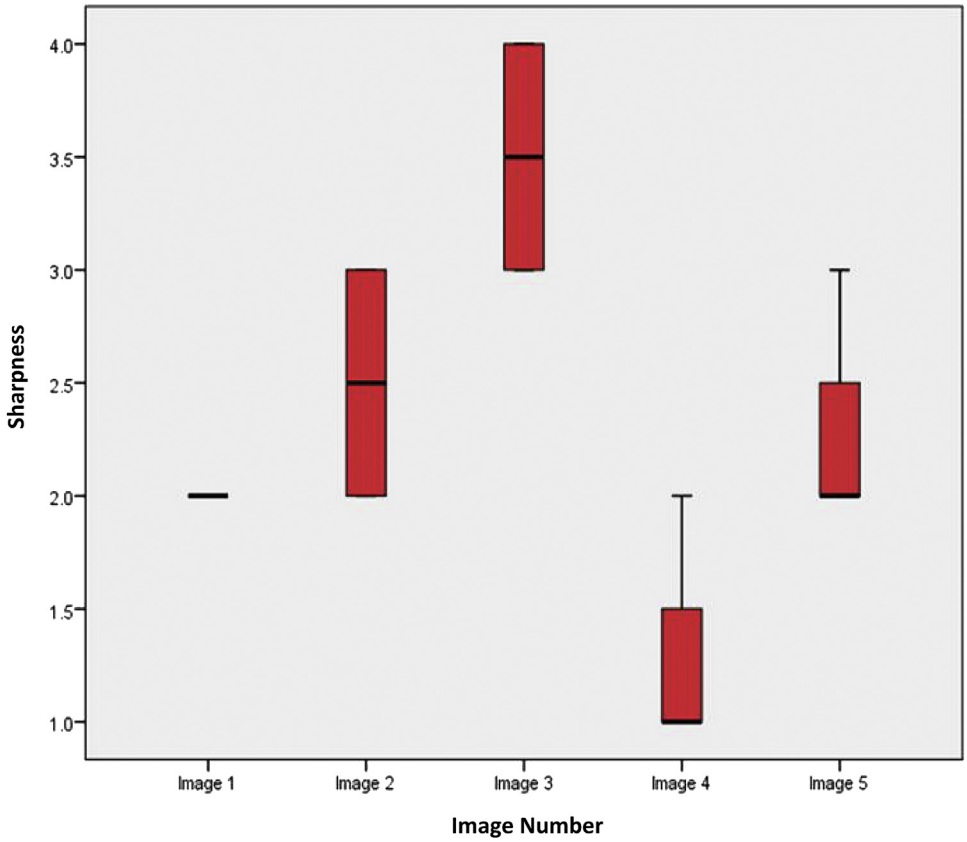

Figure 5. Differences in means for institution reference standard and optimal exposure protocols for image sharpness criteria (refer to Table 2 for exposure protocol and image randomization numbers).

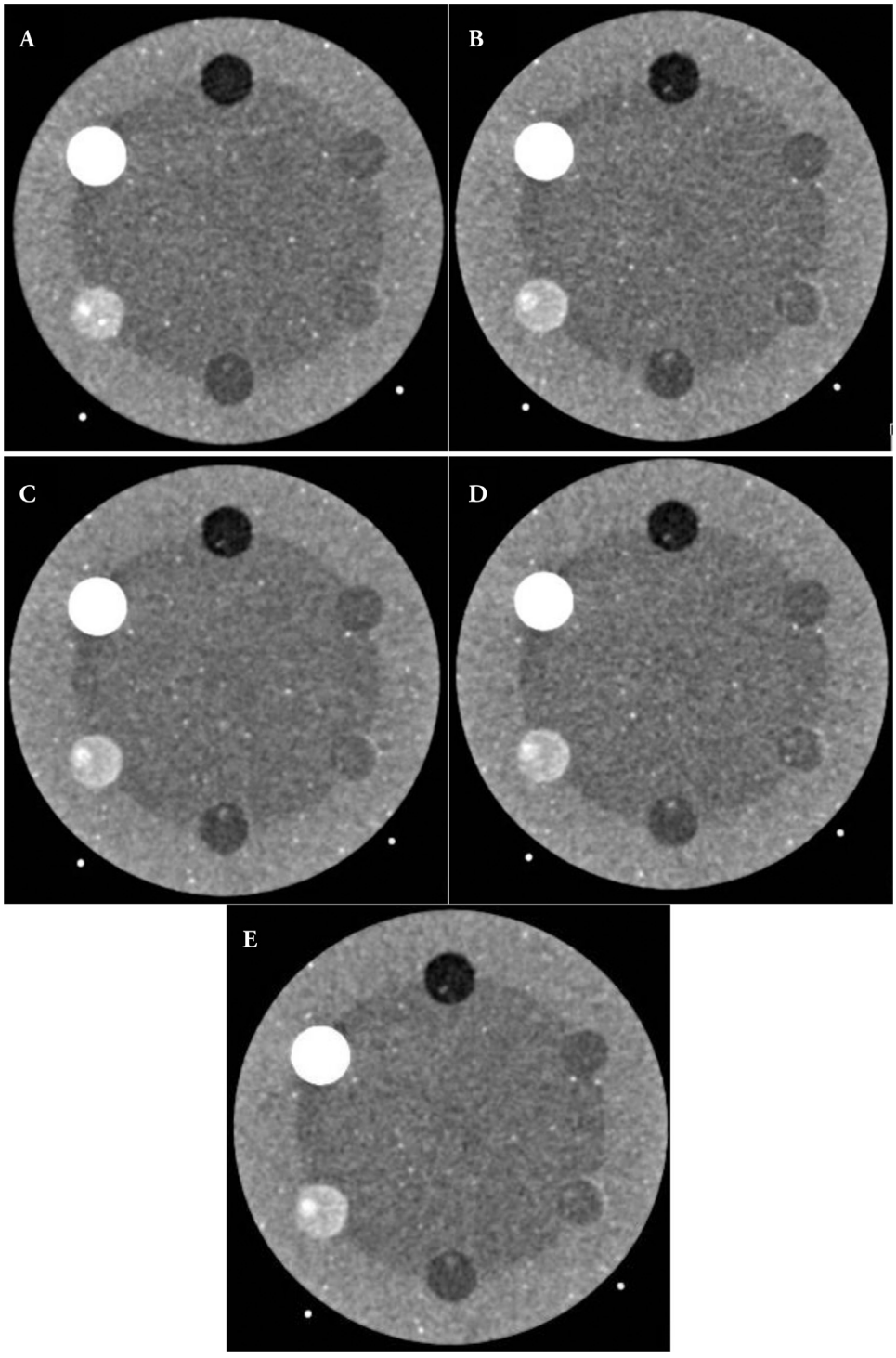

Figure 6. Images acquired from prototype phantom with institution reference standard A, 410 mAs FBP and optimized protocols; B, 370 mAs FBP; C, 310 mAs IR1; D, 330 mAs IR 2; and E, 350 mAs IR1. Refer to Table 2 for exposure protocol and image randomization numbers. FBP, filtered back projection; IR, iterative reconstruction; mAs, milliampere-second.

image reconstruction type. However, it is suggested that this is a highly subjective measure [28]. Previous studies are inconsistent with regard to the ability of IR to maintain low-contrast resolution at high strengths. The current research findings support a preference for low iteration strengths as reported in some abdominal and cranial studies [29–31]. Numerous other authors [1, 6, 27, 32–35] report the use of higher iteration strengths without loss of demarcation across multiple anatomic areas. There may be a number of reasons for opinion variation including the CT system used, the

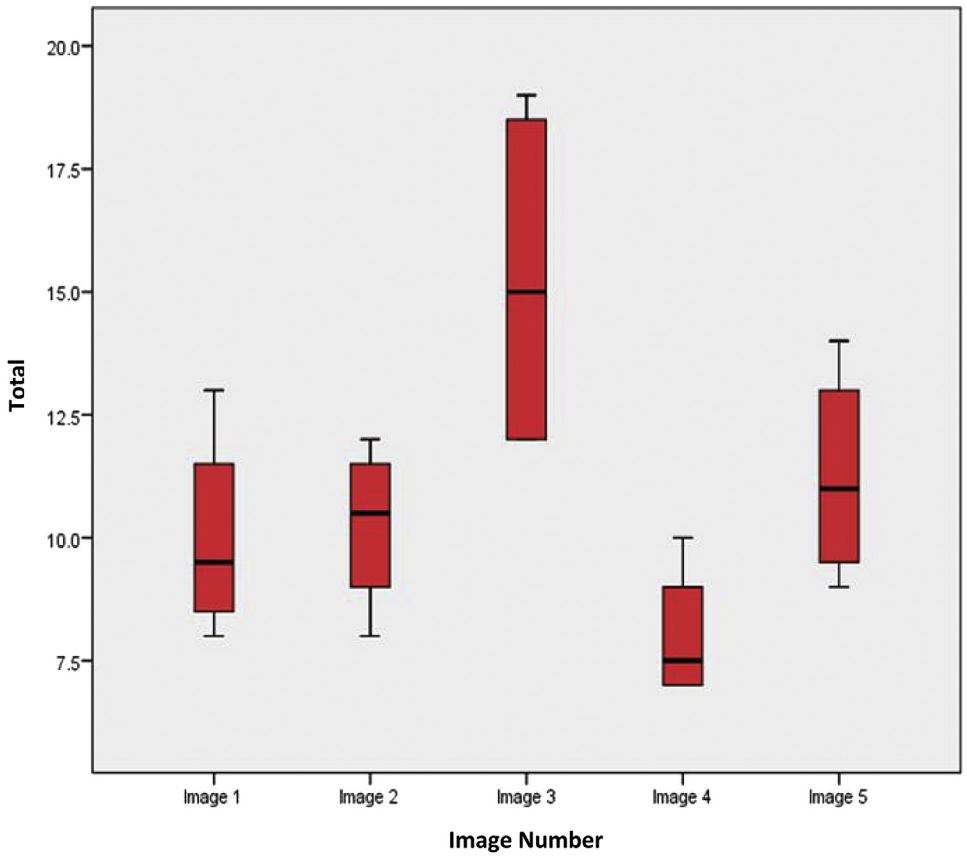

Figure 7. Total scores for the institution reference standard and optimized CT head exposure protocols. CT, computed tomography (refer to Table 2 for exposure protocol and image randomization numbers).

specific clinical task, and reviewer subjectivity and phantom studies vs. patient cohorts.

IR images are sensitive to modifications in structure edges and texture related to alterations in the spatial frequency of noise [8, 9, 10]. Visual image sharpness provided the greatest variation in image scores with a negative difference between the reference standard FBP image (for over-smoothing) and all other optimized images. The 310 effective mAs and SAFIRE strength 1 were significantly inferior to the image sharpness provided by 370 mAs with FBP reconstruction, which was considered to provide the best quality, although overall, there was no statistical difference with lower dose, low-strength SAFIRE acquisitions. As shown in the current study and suggested in previous research, these findings are likely to be linked to exposure levels and the left shift in the spatial frequency curves toward lower frequencies [5, 11].

Significant differences in scores for diagnostic acceptability, lesion conspicuity, and total diagnostic ability were evident between optimized protocols but not for diagnostic confidence in pathology visualization. Unlike previous studies [6, 9, 15, 21], significant differences were only seen when full-dose and reduced-dose FBP protocols were compared. This finding was not evident in the comparison of lower dose IR and FBP protocols, possibly due to the use of optimized low IR strengths in this study with resultant minimal alterations in noise patterns.

Limitations

Phantom studies alone cannot fully characterize CT image quality and maximum dose-reduction limits [13, 36]. The early prototype pathology phantom used in the current study is limited by the absence of a bone mimicking annulus, and therefore, there is likely underestimation of the image noise and beam-hardening artifact effect.

Image sharpness was only evaluated on a subjective basis and objective measurement of resolution using modulation transfer function could provide additional outcomes in future research. It has, however, been shown in other studies that the transverse spatial resolution is not influenced by SAFIRE regardless of density [5]. Additional limitations of the study are related to low statistical power of significant findings and the potential that the full extent of reviewer preferences may not have been shown in this small study. The results are only applicable to the Siemens equipment equipped with SAFIRE.

Conclusion

High strengths of SAFIRE have the potential to considerably influence pixel noise, CNR, and noise variance (image texture); however, systematically optimized SAFIRE protocols can maintain the diagnostic image integrity of FBP. This phantom study emphasizes that dose reduction with IR is not a simple

process; it necessitates some knowledge of IR theoretical principles; multidisciplinary experimentation prepatient implementation; and subjective image review to ensure that scan protocols are fit for purpose. This work has facilitated the local application and acceptance of lower dose head CT protocols and IR reconstruction while maintaining confidence in image interpretation. To realise the full potential of IR in head, CT requires on-going evaluation within a patient cohort to further optimize image quality and radiation dose.

Acknowledgements

The authors would like to thank Adrian Walker, Rachel Lamb, and colleagues at Leeds Test Objects Limited for development of the prototype custom-made cranial pathology phantom. Acknowledgement is also given to Dr Beverly Snaith in generation of this article.

No specific funding was received in respect of this study; however, the principle investigator was in receipt of an NIHR Masters studentship. ''This report is independent research supported by the National Institute for Health Research/Chief Nursing Officer Clinical Academic Training Programme Masters in Clinical Research Scheme. The views expressed in this publication are those of the author(s) and not necessarily those of the NHS, the National Institute for Health Research, or the Department of Health.''

References

[1] Wu, T. H., Hung, S. C., & Sun, J. Y., et al. (2013). How far can the radiation dose be lowered in head CT with iterative reconstruction? Analysis of imaging quality and diagnostic accuracy. *Eur Radiol* 23(9), 2612–2621.

[2] Haubenreisser, H., Fink, C., & Nance, J. W. Jnr, et al. (2014). Feasibility of slice width reduction for spiral cranial computed tomography using iterative image reconstruction. *Eur J Radiol* 83(6), 964–969.

[3] Brunner, C. C., Stern, S. H., Minniti, R., Parry, M. I., Skopec, M., & Chakrabati, K. (2013). CT head-scan dosimetry in an anthropomorphic phantom and associated measurement of ACR accreditation-phantom imaging metrics under clinically representative scan conditions. *Med Phys* 40(8), 081917.

[4] Nelson, R. C., Feuerlein, S., & Boll, B. T. (2011). New iterative reconstruction techniques for cardiovascular computed tomography: how do they work, and what are the advantages and disadvantages? *J Cardiovasc Comput Tomogr* 5(5), 286–292.

[5] Greffier, J., Macri, F., & Larbi, A., et al. (2015). Dose reduction with iterative reconstruction: optimization of CT protocols in practice. *Diagn Interv Imaging* 96, 477–486.

[6] Buhk, J. H., Lagmani, A., & von Schultendorff, H. C., et al. (2013). Intraindividual evaluation of the influence of iterative reconstruction and filter kernel on subjective and objective image quality in computed tomography of the brain. *Rofo* 185(8), 741–748.

[7] Grant, K., & Raupach, R. (2012). SAFIRE: Sinogram Affirmed Iterative Reconstruction. White Paper. USA: Siemens Healthcare.

[8] Rampado, O., Bossi, L., Gabrello, D., Davini, O., & Ropolo, R. (2012). Characterization of a computed tomography iterative reconstruction algorithm by image quality evaluations with an anthropomorphic phantom. *Eur J Radiol* 81(11), 3172–3177.

[9] Kofler, J. M., Yu, L., & Leng, S., et al. (2015). Assessment of low-contrast resolution for the American College of Radiology Computed Tomographic Accreditation Program: what is the impact of iterative reconstruction? *J Comput Assist Tomogr* 39(4), 619–623.

[10] Singh, S., Kalra, M. K., & Moore, M. A., et al. (2009). Dose reduction and compliance with pediatric CT protocols adapted to patient size, clinical indication, and number of prior studies. *Radiology* 252(1), 200–208.

[11] Mirro, A. E., Brady, S. L., & Kaufman, R. A. (2016). Full dose-reduction potential of statistical iterative reconstruction for head CT protocols in a predominantly pediatric population. *AJNR Am J Neuroradiology* 37, 1199–1205.

[12] Saiprasad, G., Filliben, J., & Peskin, A., et al. (2015). Evaluation of low-contrast detectability of iterative reconstruction across multiple institutions, CT Scanner manufacturers, and radiation exposure levels. *Radiology* 19, 141260.

[13] Roobottom, C. A., & Loader, R. (2016). Radiation dose reduction in CT: dose optimisation gains both increasing importance and complexity. *Clin Radiol* 71, 438–441.

[14] Zarb, F., McEntee, M. F., & Rainford, L. (2015). A multi-phased study of optimisation methodologies and radiation dose savings for head CT examinations. *Radiat Prot Dosimetry* 163(4), 480–490.

[15] McCollough, C. H., Bruesewitz, M. R., & McNitt-Gray, M. F., et al. (2004). The phantom portion of the American College of Radiology (ACR) computed tomography (CT) accreditation program: practical tips, artifact examples, and pitfalls to avoid. *Med Phys* 31(9), 2423–2442.

[16] Kilic, K., Erbas, G., Guryildirim, M., Arac, M., Ilgit, E., & Coskun, B. (2011). Lowering the dose in head CT using adaptive statistical iterative reconstruction. *Am J Neuroradiol* 32(9), 1578–1582.

[17] Smith, A. B., Dillon, W. P., Gould, R., & Wintermark, M. (2007). Radiation dose-reduction strategies for neuroradiology CT protocols. *AJNR Am J Neuroradiol* 28(9), 1628–1632.

[18] Vorona, G. A., Zuccoli, G., Sutcavage, T., Clayton, B. L., Ceshin, R. C., & Paigrahy, A. (2013). The use of adaptive statistical iterative reconstruction in pediatric head CT: a feasibility study. *AJNR Am J Neuroradiol* 34(1), 205–211.

[19] Ren, Q., Dewan, S. K., & Li, M., et al. (2012). Comparison of adaptive statistical iterative and filtered back projection reconstruction techniques in brain CT. *Eur J Radiol* 81(10), 2597–2601.

[20] Bongartz, G., Golding, S.J., Jurik, A.J., et al. (1999) European guidelines on quality criteria for computed tomography.

[21] Hara, A. K., Paden, R. G., Silva, A. C., Kujak, J. L., Lawder, H. J., & Pavlicek, W. (2009). Iterative reconstruction technique for reducing body radiation dose at CT: feasibility study. *AJR Am J Roentgenol* 193(3), 764–771.

[22] Aurumskjold, M. L., Ydstrom, K., Tingberg, A., & Soderburg, M. (2017). Improvements to image quality using hybrid and model-based iterative reconstructions: a phantom study. *Acta Radiol* 58, 53–61.

[23] Love, A., Siemund, R., & Hoglund, P., et al. (2014). Hybrid iterative reconstruction algorithm in brain CT: a radiation dose reduction and image quality assessment study. *Acta Radiol* 55(2), 208–217.

[24] Korn, A., Bender, B., & Fenchel, M., et al. (2013). Sinogram affirmed iterative reconstruction in head CT: improvement of objective and subjective image quality with concomitant radiation dose reduction. *Eur J Radiol* 82(9), 1431–1435.

[25] Bodelle, B., Wichmann, J. L., & Scholtz, J. E., et al. (2015). Iterative reconstruction leads to increased subjective and objective image quality in cranial CT in patients with stroke. *AJR Am J Roentgenol* 205(3), 618–622.

[26] Notohamiprodjo, S., Deak, Z., & Meurer, F., et al. (2015). Image quality of iterative reconstruction in cranial CT imaging: comparison of model-based iterative reconstruction (MBIR) and adaptive statistical iterative reconstruction (ASiR). *Eur Radiol* 25(1), 140–146.

[27] Brodoefel, H., Bender, B., Schabel, C., Fenchel, M., Ernemann, U., & Korn, A. (2015). Potential of combining iterative reconstruction with noise efficient detector design: aggressive dose reduction in head CT. *Br J Radiol* 88(1050), 20140404.

[28] Kalender, W.A. (2005) Computed tomography: fundamentals, system technology, image quality, applications. Erlangen: Publicis Corporate Publishing.

[29] Hardie, A. D., Nelson, R. M., Egbert, R., Rieter, W. J., & Tipnis, S. V. (2015). What is the preferred strength setting of the sinogram-affirmed iterative reconstruction algorithm in abdominal CT imaging? *Radiol Phys Technol* 8(1), 60–63.

[30] Kalra, M. K., Woisetschlager, M., & Dahlström, N., et al. (2012). Radiation dose reduction with Sinogram affirmed iterative reconstruction technique for abdominal computed tomography. *J Comput Assist Tomogr* 36(3), 339–346.

[31] Rapalino, O., Kamalian, S., & Payabvash, S., et al. (2012). Cranial CT with adaptive statistical iterative reconstruction: improved image quality with concomitant radiation dose reduction. *Am J Neuroradiol* 33(4), 609–615.

[32] Ono, S., Niwa, T., & Yanagimachi, N., et al. (2016). Improved image quality of helical computed tomography of the head in children by iterative reconstruction. *J Neuroradiology* 43(1), 31–36.

[33] Rivers-Bowerman, M. D., & Shankar, J. J. (2014). Iterative reconstruction for head CT: effects on radiation dose and image quality. *Can J Neurol Sci* 41(5), 620–625.

[34] Nie, P., Li, H., & Duan, Y., et al. (2014). Impact of Sinogram Affirmed Iterative Reconstruction (SAFIRE) algorithm on image quality with 70 kVp-Tube-Voltage Dual-Source CT angiography in children with congenital heart disease. *PLoS ONE* 9(3), e91123.

[35] Yang, W. J., Yan, F. H., & Liu, B., et al. (2013). Can sinogram-affirmed iterative (SAFIRE) reconstruction improve imaging quality on low-dose lung CT screening compared with traditional filtered back projection (FBP) reconstruction? *J Comput Assist Tomogr* 37(2), 301–305.

[36] Solomon, J., Samei, E. (2013) Are uniform phantoms sufficient to characterize the performance of iterative reconstruction in CT? Proc. SPIE 8668, Medical Imaging 2013: Physics of Medical Imaging, 86684M (March 6, 2013); http://dx.doi.org/10.1117/12.2008378.